nature climate change

LETTERS

PUBLISHED ONLINE: 10 AUGUST 2014 | DOI: 10.1038/NCLIMATE2313

Recent trends in African fires driven by cropland expansion and El Niño to La Niña transition

Niels Andela* and Guido R. van der Werf

Landscape fires are key in African ecosystems[1–3] and the continent is responsible for ~70% of global burned area and ~50% of fire-related carbon emissions[4,5]. Fires are mostly human ignited, but precipitation patterns govern when and where fires can occur[6]. The relative role of humans and precipitation in driving the spatio-temporal variability in burned area is not fully disentangled but is required to predict future burned area[7,8]. Over 2001–2012, observations indicate strong but opposing trends in the African hemispheres[4]. Here we use satellite data and statistical modelling and show that changes in precipitation, driven by the El Niño/Southern Oscillation (ENSO), which changed from El Niño to La Niña dominance over our study period, contributed substantially (51%) to the upward trend over southern Africa. This also contributed to the downward trend over northern Africa (24%), but here rapid demographic and socio-economic changes were almost as important (20%), mainly due to conversion of savannah into cropland, muting burned area. Given the economic perspective of Africa and the oscillative nature of ENSO, future African savannah burned area will probably decline. Combined with increasing global forest fire activity due to climate change[9–11], our results indicate a potential shift in global pyrogeography from being savannah dominated to being forest dominated.

Landscape fires form an integral part of the African savannah ecosystem[1]. Savannas, which evolved around 8 million years ago, mostly consist of grasslands interspersed with fire-tolerant trees[12]. In the (sub)tropics, fire occurrence in xeric savannas is limited by a lack of fuel as a consequence of reduced productivity, whereas in more mesic regions the main limitation is the short dry seasons[13]. In Africa, dry-season length gradually increases when moving away from the Equator[14]. The highest annual burned area has been observed in savannas with intermediate levels of precipitation and productivity, and distinct wet and dry seasons[13] (Fig. 1a). Most of the fire emissions originate from these savannah ecosystems on the continent[5]. Although not net contributors, African savannah fires are a source of inter-annual variability of atmospheric CO_2 concentrations and in addition emit substantial amounts of other greenhouse gases including CH_4 and N_2O (ref. 5).

On millennial timescales, burned area is thought to be largely dependent on climate and CO_2 concentrations as they drive vegetation patterns[7,15]. Although climate (mostly precipitation patterns) also plays an important role in shaping current fire regimes, human activities are also important. Humans modify the ignition probability and timing, and impact the type and amount of vegetation (fuels) available to burn, for example, by introducing cattle in the landscape[16,17]. Within African savannas, humans use fires to recycle nutrients to improve grasslands that support grazing, attract wildlife for hunting, and for agricultural purposes. Frequent fires, which reduce fuel loads, also protect settlements from occasional uncontrolled large fires[18]. Fire also plays a crucial role in the competition between woody and herbaceous species, and without the occurrence of frequent fires many African savannas might have been covered by forest[2]. Burning is thus used as an active management strategy in many African savannas[18].

Traditionally, many savannas were used for extensive grazing and hunting by their semi-nomadic inhabitants. More recently, the mobility of livestock has been reduced by ongoing socio-economic development and lack of institutional appreciation for traditional ways of living[19]. In large parts of sub-Saharan Africa, communal pastures are diminishing as a consequence of increasing population density, the introduction of land ownership and increased agricultural activity, leading to a general shift from nomadic pastoralism towards settled (pastoral) farming[19,20]. Land management is known to impact annual burned area locally[6,16,17], but the extent to which recent socio-economic developments affect annual burned area on a continental scale remains unknown. Here we study recent trends observed in African annual burned area, and disentangle the role of humans versus precipitation in driving variability in African burned area.

As a result of the large study area and spatio-temporal variability in fire occurrence, satellites are the preferred way to monitor landscape fires. The data sets from the Moderate Resolution Imaging Spectroradiometer (MODIS) instrument on-board the Terra satellite yield the highest-quality data according to assessments starting from the year 2001 (refs 21,22). The 2001–2012 observations from the MCD64A1 algorithm[22] indicate the spatial pattern in burned area (Fig. 1a) and an increase for most of southern Africa, whereas burned area decreased in northern Africa over the same time period (Fig. 1b). We developed a statistical model based on multiple linear regression (equation (1)) with precipitation (monthly Tropical Rainfall Measuring Mission (TRMM) 3B43v7 data[23]) and cropland extent (annual MCD12C1.51 data[24]) as explanatory variables to better understand their impact on the observed trends in burned area. Precipitation–burned area relations are not straightforward; increased precipitation can increase annual burned area by increasing productivity and thus fuel available for burning, or limit burned area by shortening the dry season[13,25]. Therefore, the model allows for both a positive or a negative response of burned area to precipitation variation for each grid cell (Methods; equation (2)). In addition, we explored the impact of ENSO on the observed variation in annual burned area. We focused on grid cells receiving between 400 and 1,500 mm of precipitation annually where most burned area (92%) is observed in Africa (Fig. 1a).

In southern Africa, trends in observed and modelled burned area agreed reasonably well, especially in more arid regions (for example,

Earth and Climate Cluster, Department of Earth Sciences, Faculty of Earth and Life Sciences, VU University, De Boelelaan 1085, 1081HV, Amsterdam, The Netherlands. *e-mail: n.andela@vu.nl

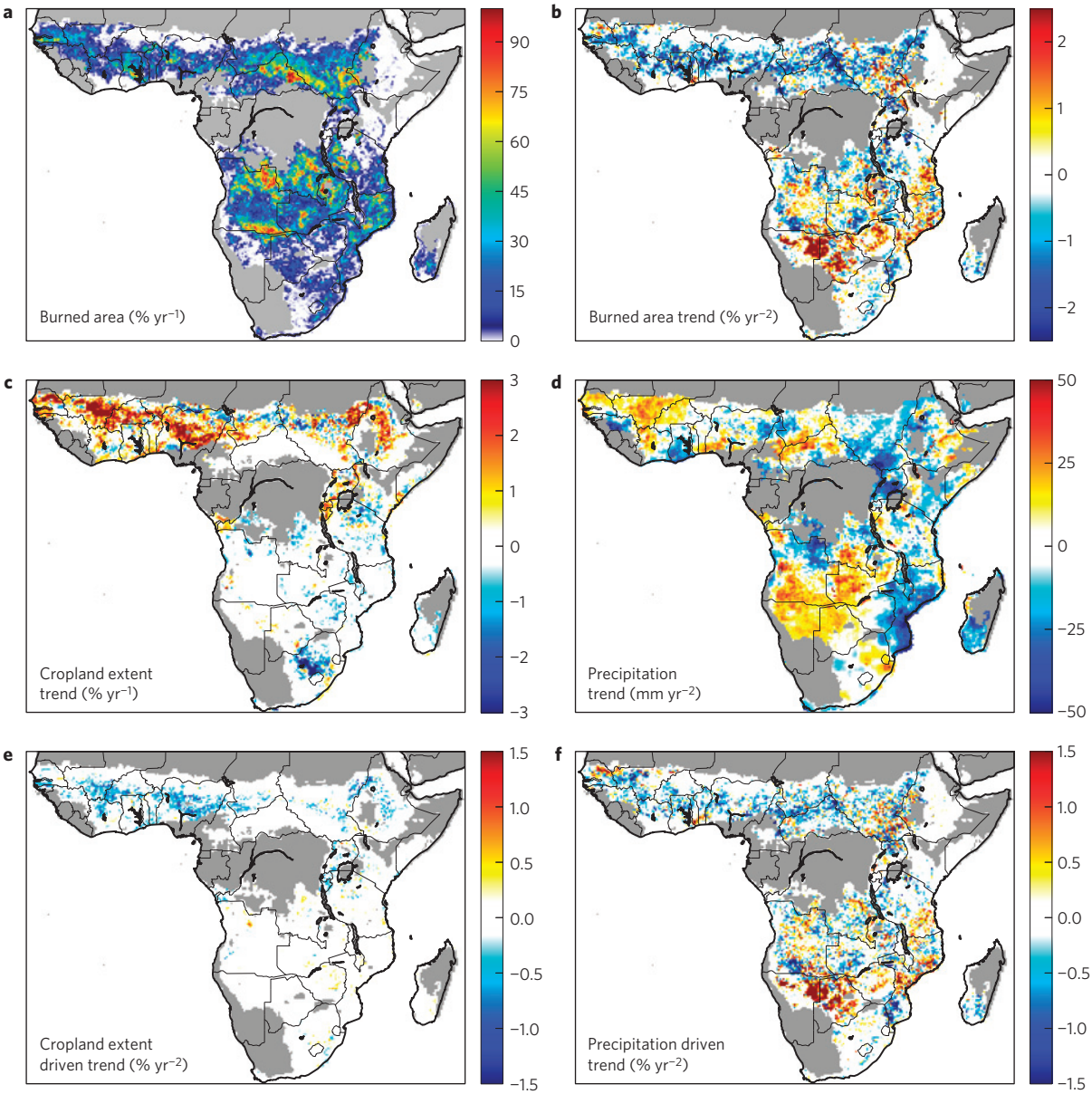

Figure 1 | Annual burned area: mean, recent trends and drivers, for areas with precipitation rates between 400 and 1,500 mm yr^{-1} based on 2001–2012 data. **a**, Observed mean annual burned area. **b**, Observed trend in annual burned area. **c**, Observed trend in cropland extent. **d**, Observed trend in precipitation. **e**, Modelled trend in burned area driven by trends in cropland extent. **f**, Modelled trend in annual burned area driven by precipitation.

Namibia and Botswana; Fig. 1b,f). A net increase in annual burned area of 10.5% was observed in southern Africa over the study period, of which about half (51%) could be explained by precipitation (Fig. 1b,f and Supplementary Table 2; Methods). In northern Africa, annual burned area declined by 25.7% over the study period. Only about a quarter (24%) of this decline could be explained by precipitation according to our model. The underlying reason behind the opposing response of burned area to changes in precipitation between southern and northern Africa is that increasing precipitation mostly occurred in more mesic parts of northern and more xeric parts of southern Africa (Fig. 1d,f).

In grid cells with high annual burned area in northern Africa, where savannas were converted into cropland, the observed decline was substantially larger than we estimated with the model based on changes in precipitation alone (Fig. 1). We estimated that about 20% of the observed decline in annual burned area over northern Africa can be explained by cropland expansion, so precipitation and land cover conversion to cropland contributed almost equally to the net decrease in annual burned area observed in northern Africa. Remaining trends may be partly caused by simplifications within the model and the short time series available, but also by second-order processes that were not incorporated in our model. Changes in land use are widespread in this rapidly changing part of the world; in about a third of the grid cells with frequent burning (defined here as having more than 10% of area burned yr^{-1}) in northern Africa agricultural area increased by more than 5% over our study period.

Additional support for the key role of socio-economic and demographic factors in driving fire variability comes from the spatial distribution of fires. The impact of conversion of savannas into agricultural land in northern Africa derived from spatial information (the annual average over our 12-year time period) is demonstrated in Fig. 2a. Particularly interesting is the sharp initial decline when agriculture is introduced in the landscape, with a stronger response than found in our model (Fig. 2b). This suggests

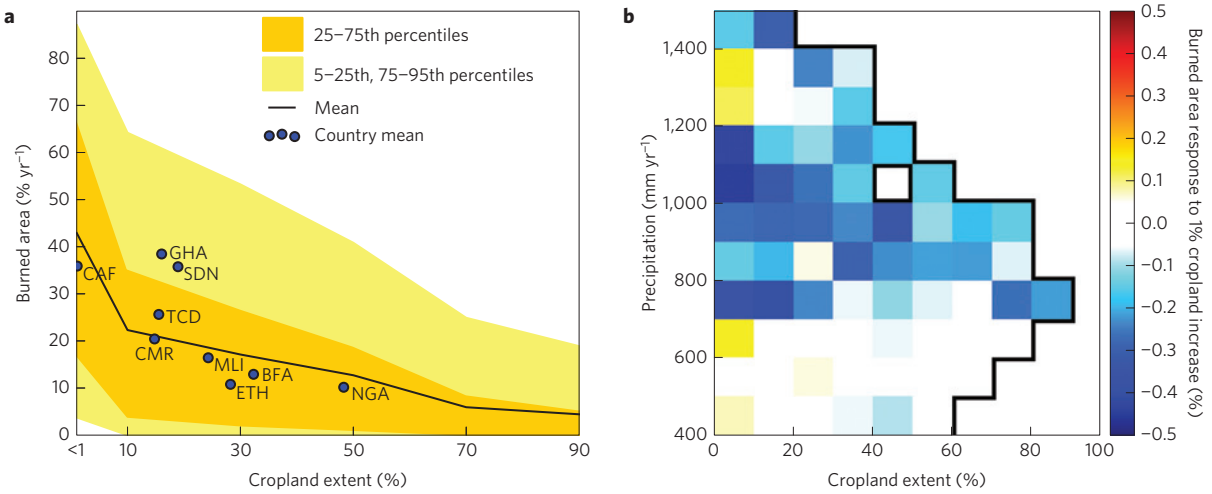

Figure 2 | Impact of cropland extent on annual burned area. a, Distribution of mean annual burned area for different cropland extent bins for northern Africa (<1%, 1–20%, 20–40%, 40–60%, 60–80% and >80%). The abbreviations indicate the mean values for various countries and include: Burkina Faso (BFA), Cameroon (CMR), Central African Republic (CAF), Chad (TCD), Ethiopia (ETH), Ghana (GHA), Mali (MLI), Nigeria (NGA) and former Sudan (SDN). Savannas were defined as land cover classes 'grassland', 'savannah' and 'woody savannah' of the University of Maryland classification (MCD12C1.51) and all grid cells were included that contained at least 90% savannah and cropland combined. **b**, Modelled response of annual burned area to a 1% increase in cropland extent for each cropland–precipitation bin based on all grid cells in the study region; bins containing less than 25 grid cells are shown in white and separated by the black line.

that our model might be on the conservative side with regard to the contribution of cropland expansion in lowering burned area (Supplementary Information). This rapid initial decline suggests that agricultural activity does not affect burned area only in the land that is actually converted, but also in the remaining savannas. Although burning continues after conversion to agriculture, large uncontrolled fires are less likely to occur owing to changes in fire management and lower fuel continuity due to, for example, more developed road networks[18]. Vegetation patterns and fire regimes are therefore likely to be affected by proximity to agricultural activity and settlements. More developed and/or densely populated savannas (for example, Nigeria and Burkina Faso) show far lower annual burned area than regions where traditional pastoralist lifestyle partly survives (for example, in Central African Republic and former Sudan; Fig. 2a and Supplementary Table 1).

Our results thus provide new evidence that part of the decline in burned area in northern Africa was caused by socio-economic developments. A key question is what caused the precipitation-driven trends, and we found that ENSO played an important role. ENSO is known to have a considerable impact on climate and vegetation growth for several African regions[26,27], and thus also on fire. The effect of ENSO on precipitation is most profound in December, January and February with lower ENSO values (La Niña) causing increased precipitation in both northern and southern Africa[27]. Southern Africa is more strongly impacted and ENSO influence continues in March, April and May[27]. To investigate the effect of ENSO on burned area, we calculated the correlation between the annual mean Multivariate ENSO Index[28] (MEI) and annual burned area anomaly (Methods). Correlation was mostly negative for southern Africa and positive for northern Africa (Fig. 3). Thus, a declining MEI (transition from El Niño to La Niña dominance) during the study period resulted in a decrease in burned area in northern Africa but an increase in southern Africa through ENSO regulating precipitation (Supplementary Information).

For Africa as a whole, over the study period the net positive trend in annual burned area caused by ENSO over southern Africa was counterbalanced by the net negative trend caused by ENSO in northern Africa. Our model estimated a 5.4% increase in annual burned area in southern Africa and a 6.2% decrease in northern

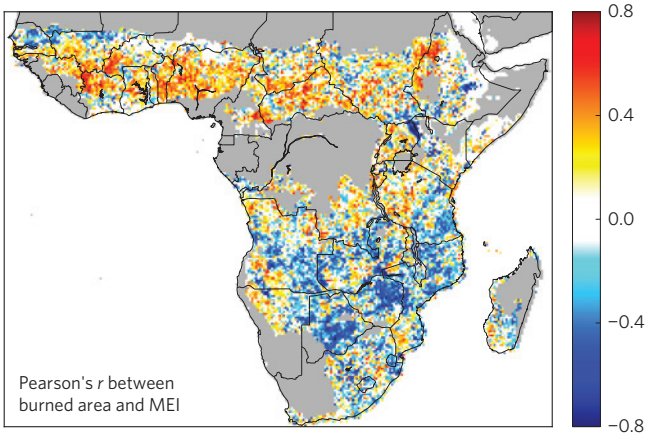

Figure 3 | Pearson's *r* between annual burned area anomaly and Multivariate ENSO Index. Regions with precipitation below 400 or above 1,500 mm yr^{-1} are masked grey.

Africa over the study period due to precipitation; total annual burned area for both hemispheres is about equal. The relation between ENSO and annual burned area depends both on the effect of ENSO on precipitation and on the antecedent precipitation–burned area response, and is further discussed in the Supplementary Information. Although we cannot conclusively attribute all variation in precipitation to ENSO alone, strong correlation between annual burned area and ENSO suggests that the possible effect of climate change was probably much smaller over the study period.

In conclusion, we are able to explain a substantial part of the opposing trends in burned area in northern and southern Africa with changes in precipitation and socio-economic changes represented by changes in cropland extent, the latter being especially important in northern Africa. The changes in precipitation were mostly related to ENSO, which moved from El Niño to La Niña dominated over the 2001–2012 period. Trends in burned area that are directly related to ENSO are cyclic (no long-term trend) and will probably shift again and have a limited effect on African annual

burned area over the next decades. For the future it is therefore likely that trends in annual burned area and fire emissions in Africa are for a large part dependent on socio-economic changes. Climate change may amplify or dampen some of these trends depending on how climate changes[7,8] but its effect for African savannas is probably smaller than the trends we found as a result of cropland expansion, especially for northern Africa. Given that socio-economic developments have been going on for several decades, it is likely that in the past burned area was considerably higher for large parts of African savannas, especially in West Africa with its relative high population density. This is in line with other studies that found that global emissions from landscape fires have been declining rather than increasing during recent history[29].

Globally, the current paradigm is that burned area is expected to increase as a result of climate change[7,8], although accounting for demographic and land use changes may suppress some of this signal[8]. The most pronounced changes are expected in the temperate and boreal regions owing to warmer conditions[9,10], and in tropical forest areas owing to drier conditions[11]. Our results indicate that in African savannas, at present responsible for most global burned area and about half of global fire carbon emissions[4,5], burned area is likely to decline in the coming decades. Northern African annual burned area has declined by more than 5% over the study period owing to land use changes that are expected to continue in the future. African population is expected to nearly double by 2050, and increasing demand for food will be met both by expansion and intensification of agriculture[30]. In the long-term, this suggests that global pyrogeography may shift from being savannah dominated to forest dominated.

Methods

Monthly burned area (BA) data[22] (MCD64A1; 08-2000 onwards) and annual land cover information[24] (MCD12C1.51; 2001 onwards) were scaled to the 0.25° resolution of the monthly precipitation data[23] (TRMM 3B43 version 7; 1998 onwards). Our study domain included all African grid cells with annual precipitation rates between 400 and 1,500 mm yr^{-1} precipitation to focus on savannah regions. We developed a statistical model that aimed to explain variability in annual BA using antecedent precipitation (API) and changes in cropland extent (dCROP) for each grid cell. As input for the statistical model, we removed the mean seasonal cycle from the BA and precipitation data (Supplementary Information). We calculated the annual BA anomaly for each grid cell not on the basis of calendar years but as the sum of the BA anomaly from 5 months before the month of peak burning until 6 months after, to circumvent issues in northern Africa where the peak fire season is in December and January. We used data from August 2000 until June 2013, resulting in 12 annual cycles for all grid cells.

Building on earlier work[25], a multiple linear regression model was used to explain the BA anomaly for each grid cell (x,y) and year (t):

$$\mathrm{BA}_{x,y,t} = \beta_i * \mathrm{dCROP}_{x,y,t} + b0_{x,y} * \mathrm{API}_{x,y,t} + b1_{x,y} + \varepsilon_{x,y,t} \quad (1)$$

where β, $b0$ and $b1$ are optimally fitted parameters to minimize the sum of ordinary least squares of the errors (ε). Positive dCROP values indicate conversion of natural vegetation into cropland. The impact of dCROP on annual BA was found to vary mostly with actual cropland extent and mean annual precipitation. To prevent overfitting we clustered grid cells into cropland extent–mean annual precipitation bins, and determined the slope β_i for each bin (i) separately (Fig. 2b). The BA–precipitation response was more variable and the slope $b0_{x,y}$ was therefore optimized for each grid cell individually. We included an intercept that varied between grid cells ($b1$) as done in ref. 25, representing the initial annual BA. Both explanatory variables are discussed below and in more detail in the Supplementary Information.

Antecedent precipitation is often thought to be the single most important driver of inter-annual variability of BA in savannas[13,25]. For each grid cell, the effect of precipitation on annual BA was explored by calculating Pearson's r between antecedent precipitation and annual BA using averaging periods from 1 up to 24 months. In general, for a given grid cell short averaging periods will be negatively correlated with BA as precipitation shortly before the burning season increases fuel moisture; whereas longer averaging periods will be positively correlated with BA through the process of fuel build-up[25]. It is therefore possible that precipitation has both a positive and a negative effect on annual burned area for each grid cell. However, we found that both effects are rarely important at the same time (~3% of the grid cells when $p < 0.1$; see Supplementary Information). Therefore, we include only one precipitation–BA response variable per grid cell in the model, based on the strongest absolute response (positive or negative). API may therefore be estimated for each grid cell (x,y) and year (t) using:

$$\mathrm{API}_{x,y,t} = \frac{\sum_{i=m-T_{x,y}+1}^{i=m} p'_{x,y,i}}{T_{x,y}} \quad (2)$$

where T is the averaging period (ranging from 1 to 24 months) for API that led to the highest absolute correlation (Pearson's r) between the running mean of the monthly precipitation anomaly p' and the annual BA anomaly and m is the month of maximum burning (Supplementary Fig. 1 and Section 2). As the effect of API may be positive or negative and is based on different T for each grid cell, we decided to optimally fit $b0$ for each grid cell. Although we used a statistical model and did not investigate underlying processes in more detail, confidence in our model may be derived from the strong correlation between API and the annual BA anomaly and from the clear spatial patterns in optimal T (Supplementary Fig. 1).

Including dCROP in the model is a logical step because the distribution of croplands has a considerable impact on current BA distribution in northern Africa (Fig. 2a), and because strong trends were observed over our relatively short study period. Owing to the limited confidence in inter-annual variation of the land cover product, we used the linear trend derived from the whole 2001 to 2012 study period.

As explained above, the short study period (2001–2012) constrains the number and ways that explanatory variables can be included in the multiple linear regression model, which is further discussed in the Supplementary Information. Trend maps (Fig. 1) are shown for all significance levels, because in general the less significant trends were part of spatial systems of significant and larger trends. Outliers may have affected some of the trends computed, especially trends observed in regions of high inter-annual climate variability, but this effect is thought to be marginal (for further details see Supplementary Information).

To investigate the role of ENSO as a driver of inter-annual variation in BA, we calculated for each pixel Pearson's r between the annual BA anomaly (as defined above) and the mean MEI index over the same period (from 5 month before the peak burning until 6 months after; Fig. 3). We then computed mean inter-annual variation separately for positively and negatively correlated areas of northern and southern Africa (Supplementary Fig. 3).

Received 16 December 2013; accepted 25 June 2014; published online 10 August 2014

References

1. Scholes, R. J. & Archer, S. R. Tree-grass interactions in savannas. *Annu. Rev. Ecol. Syst.* **28,** 517–544 (1997).
2. Bond, W. J., Woodward, F. I. & Midgley, G. F. The global distribution of ecosystems in a world without fire. *New Phytol.* **165,** 525–537 (2005).
3. Bowman, D. M. J. S. *et al.* Fire in the Earth system. *Science* **324,** 481–484 (2009).
4. Giglio, L., Randerson, J. T. & van der Werf, G. R. Analysis of daily, monthly, and annual burned area using the fourth-generation global fire emissions database (GFED4). *J. Geophys. Res.* **118,** 317–328 (2013).
5. Van der Werf, G. R. *et al.* Global fire emissions and the contribution of deforestation, savanna, forest, agricultural, and peat fires (1997–2009). *Atmos. Chem. Phys.* **10,** 11707–11735 (2010).
6. Archibald, S., Roy, D. P., van Wilgen, B. W. & Scholes, R. J. What limits fire? An examination of drivers of burnt area in Southern Africa. *Glob. Change Biol.* **15,** 613–630 (2009).
7. Pechony, O. & Shindell, D. T. Driving forces of global wildfires over the past millennium and the forthcoming century. *Proc. Natl Acad. Sci. USA* **107,** 19167–19170 (2010).
8. Kloster, S., Mahowald, N. M., Randerson, J. T. & Lawrence, P. J. The impacts of climate, land use, and demography on fires during the 21st century simulated by CLM-CN. *Biogeosciences* **9,** 509–525 (2012).
9. Kasischke, E. S., Christensen, N. L. Jr & Stocks, B. J. Fire, global warming, and the carbon balance of boreal forests. *Ecol. Appl.* **5,** 437–451 (1995).
10. Westerling, A. L., Hidalgo, H. G., Cayan, D. R. & Swetnam, T. W. Warming and earlier spring increase western US forest wildfire activity. *Science* **313,** 940–943 (2006).
11. Malhi, Y., Roberts, J. T., Betts, R. A. & Killeen, T. J. Climate change, deforestation, and the fate of the Amazon. *Science* **319,** 169–172 (2008).
12. Beerling, D. J. & Osborne, C. P. The origin of the savanna biome. *Glob. Change Biol.* **12,** 2023–2031 (2006).
13. Van der Werf, G. R., Randerson, J. T., Giglio, L., Gobron, N. & Dolman, A. J. Climate controls on the variability of fires in the tropics and subtropics. *Glob. Biogeochem. Cycles* **22,** GB3028 (2008).

14. Nicholson, S. E. & Grist, J. P. The seasonal evolution of the atmospheric circulation over West Africa and Equatorial Africa. *J. Clim.* **16,** 1013–1030 (2003).
15. Daniau, A-L. *et al.* Orbital-scale climate forcing of grassland burning in southern Africa. *Proc. Natl Acad. Sci. USA* **110,** 5069–5073 (2013).
16. Grégoire, J. M. *et al.* Effect of land-cover change on Africa's burnt area. *Int. J. Wildl. Fire* **22,** 107–120 (2013).
17. Archibald, S., Scholes, R. J., Roy, D. P., Roberts, G. & Boschetti, L. Southern African fire regimes as revealed by remote sensing. *Int. J. Wildl. Fire* **19,** 861–878 (2010).
18. Shaffer, L. J. Indigenous fire use to manage savanna landscapes in Southern Mozambique. *Fire Ecol.* **6,** 43–59 (2010).
19. Turner, M. D. The new pastoral development paradigm: Engaging the realities of property institutions and livestock mobility in dryland Africa. *Soc. Nature Resour. An. Int. J.* **24,** 469–484 (2011).
20. Tiffen, M. Urbanization: Impacts on the evolution of "mixed farming" systems in Sub-Saharan Africa. *Exp. Agric.* **42,** 259–287 (2006).
21. Roy, D. P. & Boschetti, L. Southern Africa validation of the MODIS, L3JRC, and GlobCarbon burned-area products. *IEEE Trans. Geosci. Remote Sensing* **47,** 1032–1044 (2009).
22. Giglio, L., Loboda, T., Roy, D. P., Quayle, B. & Justice, C. O. An active-fire based burned area mapping algorithm for the MODIS sensor. *Remote Sensing Environ.* **113,** 408–420 (2009).
23. Huffman, G. J. *et al.* The TRMM Multisatellite Precipitation Analysis (TMPA): Quasi-global, multiyear, combined-sensor precipitation estimates at fine scales. *J. Hydrometeorol.* **8,** 38–55 (2007).
24. Friedl, M. A. *et al.* Global land cover mapping from MODIS: Algorithms and early results. *Remote Sensing Environ.* **83,** 287–302 (2002).
25. Archibald, S., Nickless, A., Govender, N., Scholes, R. J. & Lehsten, V. Climate and the inter-annual variability of fire in southern Africa: A meta-analysis using long-term field data and satellite-derived burnt area data. *Glob. Ecol. Biogeogr.* **19,** 794–809 (2010).
26. Anyamba, A., Tucker, C. J. & Eastman, J. R. NDVI anomaly patterns over Africa during the 1997/98 ENSO warm event. *Int. J. Remote Sensing* **22,** 1847–1859 (2001).
27. Dai, A. & Wigley, T. M. L. Global patterns of ENSO-induced precipitation. *Geophys. Res. Lett.* **27,** 1283–1286 (2000).
28. Wolter, K. & Timlin, M. S. Measuring the strength of ENSO events: How does 1997/98 rank? *Weather* **53,** 315–324 (1998).
29. Marlon, J. R. *et al.* Climate and human influences on global biomass burning over the past two millennia. *Nature Geosci.* **1,** 697–702 (2008).
30. Alexandratos, N. & Bruinsma, J. *World Agriculture towards 2030/2050: The 2012 Revision* 147 (Food and Agriculture Organization, 2012).

Acknowledgements

We would like to thank P. Castellanos and A. Meesters for their helpful suggestions and all data providers and agencies for making their data publicly available. N.A. received financial support from the EU FP7 MACC-II project (contract number 218793) and G.R.v.d.W. is supported by the European Research Council (contract number 280061).

Author contributions

N.A. and G.R.v.d.W. designed the research, N.A. conducted the research, and N.A. and G.R.v.d.W. wrote the paper.

Additional information

Supplementary information is available in the online version of the paper. Reprints and permissions information is available online at www.nature.com/reprints. Correspondence and requests for materials should be addressed to N.A.

Competing financial interests

The authors declare no competing financial interests.